Review

Chinese Science Bulletin

SPECIAL TOPIC: Space Physics & Space Weather
Geophysics

April 2011 Vol.56 No.12: 1202–1211
doi: 10.1007/s11434-010-4226-9

Solar activity effects of the ionosphere: A brief review

LIU LiBo[1,2], WAN WeiXing[1], CHEN YiDing[1] & LE HuiJun[1]

[1] *Institute of Geology and Geophysics, Chinese Academy of Sciences, Beijing 100029, China;*
[2] *State Key Laboratory of Space Weather, Center for Space Science and Applied Research, Chinese Academy of Sciences, Beijing 100190, China*

Received July15, 2010; accepted September 7, 2010

Solar radiation, which varies over multiple temporal scales, modulates remarkably the evolution of the ionosphere. The solar activity dependence of the ionosphere is a key and fundamental issue in ionospheric physics, providing information essential to understanding the variations in the ionosphere and its processes. Selected recent studies on solar activity effects of the ionosphere are briefly reviewed in this report. This report focuses on (1) observations of solar irradiance at X-ray and extreme ultraviolet wavelengths and the outstanding problems of solar proxies, in the view of ionospheric studies, (2) new findings and improved representations of the features of the solar activity dependence of ionospheric key parameters and the corresponding physical processes, (3) possible phenomena in the ionosphere under extremely high and low solar activity conditions that are unique, as indicated by historical solar datasets and the deep solar minimum of solar cycle 23/24, and (4) statistical studies and model simulations of the ionosphere response to solar flares. The above-mentioned studies provide new clues for comprehensively explaining basic processes in the ionosphere and improving the prediction capability of ionospheric models and related applications.

ionosphere, solar activity, solar extreme ultraviolet, solar proxy, ionospheric index

Citation: Liu L B, Wan W X, Chen Y D, et al. Solar activity effects of the ionosphere: A brief review. Chinese Sci Bull, 2011, 56: 1202–1211, doi: 10.1007/s11434-010-4226-9

Solar activity as discussed in the scientific community can have different meanings. The first refers to the level of solar activity, indicating the intensity of solar electromagnetic radiation, particularly notable at wavelengths of solar X-rays and the extreme ultraviolet (EUV) (XUV). A second refers to solar activity events; e.g. coronal mass ejection and solar proton events. The two meanings have a close relationship as well as distinct differences. Solar activity variability and its relationship with the ionosphere have received renewed interest. In this report, we focus on recent studies of the ionosphere under different solar activity conditions and solar activity effects of the ionosphere. The features of the ionosphere during solar activity events are out of the scope of our interest here, although they are important issues in space physics and may have serious consequences on the geospace environment (e.g. geomagnetic storms, ionospheric and thermospheric storms).

*Corresponding author (email: liul@mail.iggcas.ac.cn)

The Earth's upper atmosphere absorbs solar radiation, resulting in heating, dissociation and ionization, and the ionosphere is mainly produced via the ionization effect of solar XUV. It is well established that the solar XUV fluctuates regularly and irregularly over timescales from minutes (flares) and roughly 27 days (solar rotation) to decades (11-year solar cycle), with amplitudes varying up to more than 1000 times [1–5]. Larger variability tends to occur at shorter wavelengths. The variability of the solar activity initiates huge variations in the neutral density and temperature, ion and electron densities and temperatures, neutral winds, and electric fields in the ionosphere [6,7].

Figure 1 presents the power spectra of the solar 10.7 cm radio flux index ($F_{10.7}$) and the peak electron density in the ionospheric F2 layer (N_mF2) recorded at Wuhan (114.4°E, 30.6°N) during the period of 1957–2005. The figure evidently depicts the well-known solar cycle and solar rotation variations in $F_{10.7}$ and N_mF2 at Wuhan. In contrast, N_mF2 at Wuhan varies with components much more complicated

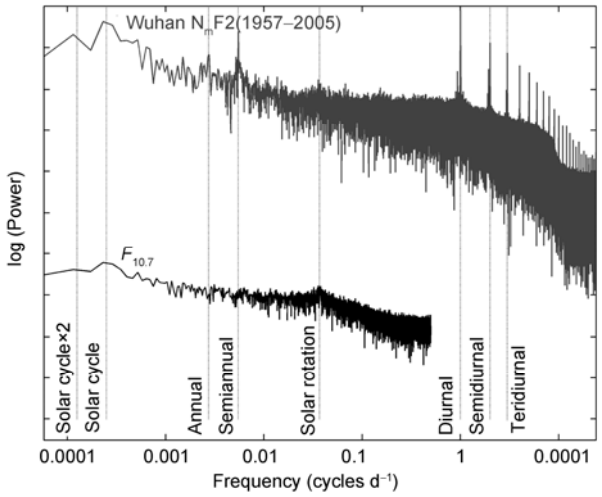

Figure 1 Power spectra of the solar 10.7 cm index $F_{10.7}$ and the peak electron density of the ionospheric F2 layer (N_mF2) at Wuhan in 1957–2005.

than those of $F_{10.7}$. This implies that the ionosphere is also substantially modified by other sources, such as the tides and planetary waves of the lower atmosphere.

The ionosphere is an open system that strongly couples with the magnetosphere and thermosphere. Various photochemical and chemical reactions and dynamical and electrodynamical processes in the system exchange and transport mass, momentum and energy in a complex manner [6]. The regular and irregular variability of solar activity affects the chemical reactions and physical processes in the system, and it further strongly modulates the structure and evolution of the ionosphere and thermosphere. It is an essential issue in ionospheric physics to study ionospheric characteristics and processes under different solar activity conditions. The study of solar activity modulation of the ionosphere will improve our understanding of the ionospheric structure and its evolution, which is critical in determining ionospheric climatology and long-term trends, and will also deepen our knowledge of chemical and physical processes in the ionosphere and thermosphere. On the other hand, the solar activity dependence of the ionosphere is one of the core issues for ionospheric empirical models. Moreover, it is realized that the ionospheric climatology, especially the solar activity effects of the ionosphere, provides an insight into ionospheric weather problems.

Over recent years, the solar activity effects of the ionospheric parameters have received renewed interest, and considerable progress has been achieved. In this brief review, we focus on four aspects: (1) observations of the solar irradiance and outstanding problems in solar proxies; (2) novel and detailed features of solar activity dependence of ionospheric parameters at different altitudes; (3) the possible states of the ionosphere under a condition of extreme solar activity; and (4) the response of the ionosphere during solar flares. Priority is given to works carried out by Chinese scientists.

1 Solar radiation observations and solar proxies

The spectrum of solar XUV radiation and its time evolution are essential in investigating the ionosphere and thermosphere. Solar XUV is nearly totally absorbed before it enters the lower atmosphere. Consequently, solar X-rays and EUV cannot be reliably monitored with ground-based instruments. Solar XUV fluxes were measured by rockets and satellites and estimated using indirect methods. Unfortunately, space-based measurements of solar XUV have been intermittent for more than two decades.

Solar XUV flux data from the observations of rockets and Atmosphere Explorer satellites have been collected to provide a fundamental database for the solar XUV spectrum and empirical models [8]. In recent years, solar XUV observations made by NOAA/GOES, Yohkoh/SXT, SNOE/SXP, SOHO/SEM, and TIMED/SEE as well as those made on board several rockets have enriched our understanding of the solar spectral structure and its temporal variability [9–13]. Atmosphere Explorer and Solar Heliospheric Observatory (SOHO) satellites continuously measured solar fluxes for the longest durations [14]. Since 1996, solar EUV fluxes in 26–34 nm and 0.1–50 nm wavelength ranges were continuously monitored by the Solar EUV Monitor (SEM) spectrometer aboard SOHO, which provides an unprecedented opportunity for ionospheric studies. Detailed information on solar XUV observations can be found in published works [5,15].

Several empirical models [8,15–17] have been developed to quantify wavelength-dependent changes in solar EUV irradiance. Among these empirical models, HFG [8], EUVAC [10] and its high-resolution version HEUVAC [11], and EUV97 and its updated version Solar2000 [15] are widely used for aeronomic calculations.

Unfortunately, solar XUV observations are generally conducted over short periods and intermittently owing to their expense. Direct measurements of the solar XUV spectrum and its variability are not available for most times. In the absence of direct EUV observations, we rely on solar proxies to indicate the intensity of solar activity [5,18]. Solar indices, which are well known and commonly used, include the sunspot number R, the solar radio flux at 10.7 cm wavelength $F_{10.7}$, He 1083, and the MgII core-to-wing index [12,18–22]. These indices are distributed by international institutions and are easily available from websites. The longest data series among these indices is the sunspot number, which has been recorded routinely for over 400 years. The next longest data series is that of $F_{10.7}$, which has been almost continuously recorded since the first observation in 1947. There are at least two justifications for using solar proxies to indicate solar activity. Firstly, there is high

correlation among levels of radiation originating from different solar atmospheric regions; that is, the sunspot number, $F_{10.7}$, and solar EUV are highly correlated in a statistical sense [10,11,15]. Secondly, the sunspot number and $F_{10.7}$ are routinely monitored on the ground. A set of solar radiation lines (e.g. the He I 1083 nm and Mg II core-to-wing ratio based on the spectral structure around 280 nm) is recommended to measure the level of solar irradiance [12,13], since the lines have strong correlation with the intensity of solar EUV flux [5,12,13]. Unfortunately, they are not widely used yet.

Doubts have arisen with respect to the feasibility of solar proxies as a quantitative representation of solar XUV flux. There have been many attempts to test the effectiveness of different solar indices. Particularly, the yearly average values of the relative sunspot number were widely used to indicate solar activity in early ionospheric research and empirical models. Later works revealed that $F_{10.7}$ has obvious advantages over the sunspot number in representing solar EUV. On the other hand, statistical analysis shows that both the sunspot number and $F_{10.7}$ follow the amplitude of solar EUV in a nonlinear way [8,10]. Moreover, the solar proxies and EUV are not well correlated on short-term scales [17] (e.g. the day-to-day variation) mainly because solar radiation at different wavelengths originates from different sources. Thus, remarkable discrepancies are expected in their temporal evolution features. It has long been realized that neither the sunspot number nor $F_{10.7}$ is ideal for representing solar EUV variability accurately. Recently, modified solar proxies (e.g. $E_{10.7}$ and $F_{10.7P}$) have been proposed. $E_{10.7}$ [15,19] is designed to scale the total EUV energy arriving at the top of the Earth's atmosphere in the units of $F_{10.7}$. On longer temporal scales, $E_{10.7}$ and $F_{10.7}$ are highly correlated [19], and $E_{10.7}$ is nearly identical to $F_{10.7}$. $E_{10.7}$ takes account of the heating effect of the upper atmosphere and is designed to improve thermospheric density modeling [15]. Another new proxy is $F_{10.7P} = (F_{10.7} + F_{10.7A})/2$, which was developed based on daily $F_{10.7}$ and its 81-day moving average value, $F_{10.7A}$. $F_{10.7P}$ has been used as a solar EUV proxy in solar irradiance empirical models (e.g. HFG and EUVAC) [8,10] and ionospheric investigations. Utilizing the SOHO/SEM EUV records, Liu et al. [23] further confirmed that $F_{10.7P}$ represents fairly well the intensity of solar EUV flux [8,10]. Therefore, $F_{10.7P}$ is recommended as a better solar proxy for common use in that it retains the advantages of $F_{10.7}$ of a long-term record and good availability.

Besides various attempts to retrieve solar proxies directly from solar data, several ionospheric indices have been successively introduced since the 1950s [18,24–27]. These indices are deduced from ionospheric data measured at single stations or over regions. The superiority of ionospheric indices over solar indices in representing changes in ionospheric parameters has been validated. Representative ionospheric indices are IG_{12} [24], the Australian T index, and MF_2 [26]. These indices are based on the monthly median foF2. It is well established that the E-layer critical frequency foE closely follows the variation of solar zenith angle; thus, useful solar EUV information can also be estimated from foE [28]. Furthermore, it is worth mentioning that the regional and global mean ionospheric total electron content (TEC) [29–31] can well capture the variability of solar irradiance with the outstanding advantage of the global coverage of the global positioning system (GPS)-derived TEC. Similar works involve deducing an ionospheric index to drive ionospheric models for regional predictions with data from ionosondes [18,32]. The aforementioned works may lead to potential applications in monitoring and forecasting space weather and improving ionospheric models.

It is essential to predict the solar activity accurately, especially the trend of the sunspot cycle. Nowadays, popular prediction approaches include the neural network approach, similar-cycle method, empirical orthogonal decomposition, and wavelet analysis [33]. The properties of upcoming solar cycle 24, especial the intensity and peak time, have been forecast. It is interesting and surprising that the predicted results conflict; some articles predict solar cycle 24 to be a period of low solar activity [33] while others predict it to have a peak in solar activity that is 30%–50% higher than the peak of the current cycle [34]. The huge discrepancies indicate that the prediction of solar variability is still an unresolved topic posing a great challenge to researchers.

2 Characteristics of the solar activity dependence of the ionosphere

2.1 Features around the F2 peak

The ionospheric electron density is highest around the F2 peak, and thus, the F2 peak has been the subject of many investigations. The solar activity dependence of ionospheric F2 parameters has been studied for a long period. The critical frequency of the F2 layer (foF2) or peak density (N_mF2) [23,35–44], peak height (h_mF2) [6,23,40], TEC [29–31, 45–51], plasma temperature and scale height [40,51], and thermosphere winds [52–55], temperature and neutral compositions [55–57] have been recently invest- igated. These studies mainly discussed the complicated trends and sensitivity of the solar activity dependency of the ionosphere, the detailed features and physical processes, and how to represent those characteristics effectively in applications.

As mentioned above, the sunspot number R and $F_{10.7}$ have been traditionally used in ionospheric studies. Most early studies on the solar cycle effects analyzed ionospheric data taken from few stations over a short period. Furthermore, these results are limited to periods with values of $F_{10.7}$ rarely exceeding 200 sfu (solar flux units; 1 sfu = 10^{-22} W m^{-2} Hz^{-1}). The relationship between the TEC (or N_mF2) and $F_{10.7}$ (or R) was reported to be linear by early works. A nonlinear dependence of the ionospheric parameters on solar proxies was discovered in latter studies [35–38,58,59].

For example, Balan et al. [58] and many others reported that the TEC and N_mF2 linearly increase with solar proxies at low and moderate solar activity levels, but the linearity breaks down at a higher activity level at all stations. The values of TEC and N_mF2 no longer increase (and even decrease) at higher solar activity levels at some stations, indicating saturation.

It is still controversial whether the saturation is a true manifestation of the solar activity dependence of the ionosphere. If it is true, what is the key factor? Balan et al. [58–60] showed that there is no ionospheric saturation effect for the TEC and N_mF2 against solar EUV, and further stated that the saturation feature is the result of the nonlinear variation in the solar EUV with $F_{10.7}$. In contrast, Liu et al. [35] found that there is an foF2 saturation effect with EUV radiation and it is more significant in equatorial anomaly regions. They thus postulated that the daily ionospheric equatorial fountain and pre-reversal enhancement contribute largely to the saturation. Liu et al. [23] carried out an analysis based on a longer series of daily solar EUV data recorded by SOHO/SEM and N_mF2 data recorded at 20 ionosonde stations in the East Asia/Australia sector. The objective of their work was to quantify the solar activity sensitivity of daytime N_mF2 in the East Asia/Australia sector and to evaluate the dynamic effects and atmospheric consequences on the solar activity effects of N_mF2. Remarkable latitudinal and seasonal differences were illustrated in the sensitivity of the response of N_mF2 and electron density at given altitudes to solar XUV [23,31,60]. Liu et al. [23] reliably confirmed that the nonlinearity of the solar EUV against $F_{10.7}$ itself is not enough to explain the ionospheric saturation effect, and found that dynamic and chemical processes determine the seasonal and latitudinal features of the saturation effect. Kane [14] reported that solar EUV increased 150% from 1996 to 2000, and N_mF2 changed 210%–290% at seven stations. He found that the solar EUV changes themselves were insufficient to account for the observed changes in N_mF2. In fact, current ionospheric theoretical models can reasonably reproduce the observed latitudinal and seasonal differences [23,31,60] if the solar activity effects of neutral compositions and chemical and dynamical processes are consistently included in the models; this further indicates that the solar activity not only determines the photoionization rates but also modulates various factors and processes in the geospace system.

One exciting finding from recent investigations is that the solar activity effects of global TEC and nighttime N_mF2 have linear, saturation and amplification features. The detailed trends are found to be dependent on latitude, local time and season [30,37,48]. The solar activity variation in nighttime N_mF2 at some stations retains the daytime saturation feature in summer, has a linear feature during the equinoxes, and has an amplification feature in winter. Chen et al. [37] stated that dynamical processes (pre-sunset enhancement of the equatorial E×B vertical drift and neutral winds) and changes in neutral compositions contribute to the seasonal difference in the solar activity effects of nighttime N_mF2. Liu et al. [48] provided a quantitative description of the three kinds of solar activity effects in the global TEC. They illustrated the local time variation and longitudinal distributions of the TEC solar activity sensitivity in the four seasons. The saturation is found to cluster in equatorial anomaly regions. The results are supported by Ma et al. [61], who used ionosonde N_mF2 data to show latitudinal double peaks in the nonlinear coefficient of N_mF2 versus solar proxies.

Liu et al. [30] analyzed the JPL GPS-TEC data over one solar cycle to explore the overall climatological features of the ionosphere. The mean TEC data are averaged globally and over low-, middle-, and high-latitude bands in the southern and northern hemisphere, separately, and both hemispheres together. There is stronger solar activity sensitivity in lower latitude bands, and the saturation effect in the mean TEC versus $F_{10.7}$ is more pronounced at low latitudes, while the mean TEC increases more rapidly for higher solar EUV fluxes. These mean TEC data, compared with individual TEC data, capture more obviously the different time-scale variations in the solar activity because local noise is effectively reduced [1,14,22].

The "hysteresis" phenomenon is an unresolved problem [41,46,62,63]. Similar to the "hysteresis" effect for magnetic materials, foF2 may have different values at the same solar level during different phases of a solar cycle. There is not yet an accepted explanation for the "hysteresis" effect. Mikhailov et al. [41] postulated that the effect is associated with differences in the geomagnetic activity during the ascending and descending phases. It is known that geomagnetic activity is generally stronger during the descending phase than during the ascending phase. Kane [21] attributed the effect to the delayed response of solar EUV to the change in $F_{10.7}$. Attempts have been made to include the possible influence of the historical solar activity state on the ionosphere in ionospheric models [36]. The "hysteresis" effect, however, is difficult to reproduce effectively in models, which is one of the key problems in long-term predictions of the ionosphere.

The relationship between foF2 and solar indices is critical in ionospheric empirical models. A linear pattern is used in some models. In contrast, the international reference ionospheric model IRI [18] adopts a two-segment linear model to simulate the solar activity dependence of electron density. A threshold of the yearly moving-average $F_{10.7}$ or sunspot number is empirically set. In the IRI model, N_mF2 increases linearly with the solar index before the threshold is reached, while it is constant afterward. Renewed investigations validated that the solar activity effect of the ionosphere can be well presented by a quadratic pattern [48]. A higher-order polynomial does not effectively improve the fitting [64]. Thus, we strongly recommend a quadratic

polynomial be adopted in future ionospheric models.

On the other hand, changes in thermospheric compositions (e.g. the ratio of [O]/[N_2]) substantially affect the ionosphere. The neutral density and temperature in the thermosphere increase with the level of solar activity [56,56] owing to the increase in solar UV heating and ion drag. Hedin [65] found higher correlation between the neutral density and solar EUV than between the neutral density and $F_{10.7}$. Furthermore, a double-peak latitudinal structure, similar to that of the equatorial ionization anomaly, is apparent in the thermospheric total mass density measured by the CHAMP satellite at 400 km [66]. The double-peak structure is more apparent for higher solar activity. In addition, vibrationally excited N_2 greatly increases at solar maximum, which leads to a higher recombination rate of O^+. Calculation results [43,67] also show that vibrationally excited N_2 may strengthen the nonlinear feature of N_mF2 with $F_{10.7}$.

The thermospheric temperature varies with the level of solar activity, which is reflected in h_mF2 and electron density profiles. Taking Wuhan for example, h_mF2, the bottomside profile parameter B0, and the scale height deduced from ionosonde profile observations increase with solar activity [23,68]. Similar characteristics have been reported in the incoherent scatter radar data recorded at Arecibo and Millstone Hill [40,51]. Naturally, neutral winds play important roles in the ionosphere changes. During the daytime, enhanced poleward winds decrease the F2 peak height, accelerate the recombination loss, and further decrease electron density. Unfortunately, the direct observations of neutral winds are difficult and not yet available globally. On the other hand, the h_mF2-derived results [52–54] show that the meridional wind at middle and low latitudes, and especially its diurnal amplitude, weakens with solar activity. Moreover, the equatorial vertical drift induces the daytime fountain effect, which is the most important dynamical process in the low-latitude ionosphere. Measurements made by satellites and incoherent scatter radars reveal that vertical drift is often strongly enhanced around sunset and has a linear trend with $F_{10.7}$ [69]. The sunset pre-reversal enhancement of the vertical drift has important consequences, resulting in a much longer duration of the nighttime equatorial anomaly at solar maxima [66].

2.2 Features at different altitudes

An ionosonde may provide information on the bottomside ionosphere, and GPS receivers register the integrated electron density along the path of the radio signal. The topside ionosphere is detected by incoherent scatter radars and satellites. The topside ionosphere is closely coupled with the plasmasphere via chemical exchanges (i.e. $O+H^+ \leftrightarrow O^+ + H$, $He^+ + N_2 \rightarrow N^+ + N + He$). The plasma and energy are injected into the plasmasphere from the topside ionosphere during the daytime, and they return to the topside ionosphere at night. With increasing solar activity, the O^+–H^+ transition height moves upward, indicating variations of the topside ion compositions (O^+, H^+, He^+ and N^+) at given altitudes [70–74]. Therefore, it is possible that light ions are dominant at solar minima but give way to O^+ ions at solar maxima at some altitudes. In other words, the upper transition height (i.e. the altitude with the same concentrations of O^+ and light ions) becomes higher. Zhao et al. [74] examined the seasonal and solar activity variations of the plasma compositions at 800 km and developed an empirical model for the DMSP plasma density using empirical orthogonal functions. Liu et al. [75,76] further studied the topside plasma density of the DMSP observations and found interesting climatological features: in the topside ionosphere there is strong annual asymmetry in the yearly variations, and an amplification effect in the solar activity dependence of the plasma density was reported for the first time.

Investigation of the solar activity effects of the ionosphere at different altitudes will improve our understanding of variations of the ionosphere and its chemical and dynamical processes. Su et al. [77] analyzed the electron density data measured by the Japanese incoherent scatter radar to investigate the altitude dependencies of solar activity variations of the ionospheric electron density. The observations show strong altitude differences. Electron density at altitudes below 300 km increases nonlinearly with $F_{10.7}$. The nonlinearity weakens with altitude. The electron density above 450 km is found to vary linearly with $F_{10.7}$.

The topside plasma density profiles can be described with h_mF2, N_mF2, and the plasma scale height [66,76] under the diffusion equilibrium assumption. The scale height is a key parameter for the topside ionosphere [73], and it provides clues in studying the ionospheric structure and its dynamical processes. Peak parameters (h_mF2, N_mF2) and scale height can be retrieved from electron profile measurements of the incoherent scatter radars. The profiles are fitted with a Chapman profile function with an altitude-varying scale height. Lei et al. [40] and Liu et al. [51] analyzed systematically the historical records of electron and ion temperature and electron density profiles observed by the Arecibo and Millstone Hill incoherent scatter radars. Distinct diurnal and seasonal variations were found in the ionospheric scale height. The scale height tends to increase linearly with solar activity, which is associated with the thermal structure and dynamical processes. They also presented the statistical relationship between the scale height and other parameters, which may guide modeling of the ionospheric profiles.

The increase in plasma density with solar EUV at 800 km differs from the MU radar results. The former shows an amplification feature [75]. Moreover, the seasonal variation of the plasma density at 800 km is dominated by the annual component. The annual asymmetry strengthens at higher solar activities [74,76]. It is unexpected that the plasma density at 600 km measured by the ROCSAT-1 satellite has linearity, saturation, and amplification trends as the solar

activity increases [66]. There is a distinct equatorial anomaly in the plasma density at 600 km around the sunset for periods of high solar flux, which also indicates enhancement of the equatorial vertical drift. It is interesting that the electron density saturates at lower altitudes; e.g. at 400 km [66].

Liu et al. [48,75] and Chen et al. [67] proposed an explanation for the three kinds of solar activity dependencies of the TEC and electron densities at different altitudes. The complicated solar activity effects of the ionosphere can be understood if the variations of the key parameters (N_mF2, h_mF2 and scale height) are known. According to their scheme, at high altitudes (e.g. 800 km), the most important factor is the scale height, which determines the amplification, and at ROCSAT-1 altitudes, the plasma density is controlled by all three parameters. The solar activity effect in equatorial regions is strongly modulated by the variation of h_mF2, showing remarkable latitudinal differences.

Rich et al. [78] studied the influence of solar rotation on the topside plasma density and temperature. Compared with the peak region, the topside ionosphere has stronger solar rotation modulation. As mentioned above, there is also strong 27-day modulation of the mean TEC averaged globally and over different latitude bands [29–31].

3 The ionosphere under extreme solar conditions

The variability of solar activity itself is an elusive topic. According to historical sunspot records, virtually no sunspots were observed during the Maunder Minimum period (1645–1715). Reconstructed records of the cosmogenic isotope ^{14}C and tree rings suggest the Grand Maximum, a period of intense solar activity during 1100–1250 [79]. Furthermore, the solar activity during 2007–2009 was extremely low and one of the longest recent solar minima. This gives rise to speculation of prolonged low solar activity such as the Maunder Minimum. The international campaign "Deep Solar Minimum" has been proposed to investigate the characteristics of the space environment under conditions of extremely low solar activity and its possible influences on global warming. The unusual behaviors and processes of the ionosphere and thermosphere certainly deserve close attention.

Smithtro et al. [80] constructed the solar irradiance under extreme solar activity conditions via separating and extrapolating coronal and chromospheric emissions. The reconstructed solar irradiance was input to a one-dimensional global average ionosphere and thermosphere model to simulate the upper atmosphere behaviors at different solar activity levels. Their results showed that, at extremely low solar activity levels, the neutral temperature and h_mF2 decline as the solar EUV flux decreases. The lower temperatures imply higher N_2 and O_2 concentrations at F2 peak altitudes, inducing a lower N_mF2 and the ratio of O^+ to molecular ions. The feature is somewhat similar to the G conditions during some geomagnetic storms. On the contrary, there is an amplification effect in the case of extremely high solar activity [80], which is similar to that of the mean TEC with solar EUV [30]. Additionally, the ionosphere was investigated for the period 2007–2009 using measurements of the electron density and thermospheric density made onboard CHAMP and GRACE satellites. In particular, the thermospheric density at 400 km was found to be unusually low by 30%. These results are fascinating, although they await publication.

A novel finding is that, in the absence of solar EUV, the value of TEC is negative if the observed fitting relationship is extrapolated to the lowest limit [30]. Naturally, it is impossible for TEC to be negative. However, it suggests that under extremely low solar activity, the ionospheric physical processes should be unique and differ from those of the normal conditions. Unknown issues include the solar spectrum under these extremes, the state of the ionosphere, and its dominant physical processes. More importantly, the impacts on our global climate system need to be determined.

Extreme solar events often accompany strong solar activity. Many serious events (e.g. the 1989 events, the 2000 Bastille Day event, the October–November 2003 storms [81], and the 1859 event [82]) have been reported in the literature. Although there are innumerable case studies and statistical studies on ionospheric storms, it remains difficult to reliably predict the accurate evolution of the ionosphere when a serious solar event erupts. An extreme storm occurred on September 1, 1859, with $\Delta H = -1600$ nT recorded at Mumbai, India. Unfortunately, we do not know what will happen if an event of such strength or an even stronger event reaches the Earth.

4 Response of the ionosphere to solar flares

A solar flare is a sudden brightening of radiation in solar active regions. Solar flares occur frequently in solar maxima years. During solar flares, huge energy is abruptly released from the Sun, inducing enhancements with varying amplitudes at radio, visible light, and XUV wavelengths with durations ranging from about 10 min to hours [83]. Explosive radiation propagates at light speed and strikes the Earth after 8 min. The flares abruptly change the structure and state of the ionosphere and thermosphere in the sunlit hemisphere, causing sudden ionospheric disturbances [84]. The disturbance phenomena include sudden cosmic noise absorption induced by sudden electron density enhancement in the D region, short-wave fadeouts, sudden phase anomalies, sudden frequency disturbances, magnetic solar flare effects, and a sudden increase in TEC (SITEC) [85].

The ionospheric response to solar flares has been widely studied with multiple instruments since the 1960s. Davies et

al. [84] summarized the sudden disturbance phenomena during solar flares. Many previous works concentrated on very intense flares observed at a limited number of stations. With the advent and popularity of GPS technology, GPS-TEC became a suitable parameter to effectively monitor SITEC and the overall eruptions of flare radiation. The advantage of GPS-TEC is its high accuracy and its outstanding spatial coverage and temporal continuity. GPS-TEC is ideal for monitoring ionospheric disturbances during solar flares in space weather applications.

In recent years, many scientists studied global variations of SITEC during solar flares [86–98]. Representative findings include (1) that GPS-TEC is very sensitive to solar flares, and can be used to monitor M+-class flares, (2) that the conclusion of no correlation between the TEC increments and solar zenith angles [85] is incorrect, and (3) that a strong response is also registered in the thermospheric density [88].

Zhang and Xiao [95] analyzed the GPS-TEC recorded at 53 stations for the April 15, 2001 flare and found a negative correlation of SITEC with the solar zenith angle. Wan et al. [86] stated that the time rate of the flare-induced TEC increment is proportional to the effective flare radiation flux and inversely proportional to the Chapman function associated with the solar zenith angle. Their result was validated with the GPS-TEC data recorded during the July 14, 2000 flare. Chen et al. [89] statistically investigated the X-class intensive flare events during 1996–2003 and found a negative relationship between the TEC increment and solar-terrestrial distance and flare duration. The results of Zhang and Xiao [91–94] show asymmetry of the absolute TEC increment about local noon; that is, the flare-induced TEC increment is greater in the afternoon than in the morning in summer, and the reverse in winter and during the equinox. Moreover, the response is dependent on the flare location on the solar disc [83,92]. Zhang et al. [92] found a larger SITEC for a flare at a lower heliographic longitude. However, it is unclear how the response of the ionosphere is determined by the heliographic position of the flare.

Hitherto, there have been few simulations of the flare effects of the ionosphere. Le et al. [97] developed a simple model for solar radiation in the course of flares and calculated the response to the X17.2 solar flare on October 28, 2003 using a one-dimensional theoretical ionospheric model. Their calculations validated the strong control of the solar zenith angle over the ionospheric response to flares. The observed seasonal and local time dependences of the flare effects of the ionosphere are also reproduced in their modeling. From XUV observations, Huba et al. [98] made the first global simulation of the ionosphere response for the July 14, 2000 flare, and Meier et al. [99] simulated the evolution of the ionosphere during this event and evaluated the XUV at different wavelengths.

There has been recent interest in the thermosphere response to flares. The traditional view is that the time constant of the neutral atmosphere is large, and thus the thermosphere responds slowly to the rapidly varying XUV in the course of a flare. Sutton et al. [100] reported the first measurements of the thermosphere neutral density response to the October 28, 2003 X17.2 and November 4, 2003 X28 flares. The density measurements were provided by accelerometers on the GRACE and CHAMP satellites at altitudes of about 490 and 400 km, X-ray fluxes by GOES-12, and EUV fluxes by the SEE instrument on TIMED. The exosphere temperature increases were estimated to be 125–175 K and 100–125 K, respectively. It is strange that the thermosphere density at low to middle latitudes increased about 50%–60% in 72±47 minutes in the first case and 35%–45% in the second case. The observation challenges our current understanding of the mechanisms governing the thermosphere.

Solar energetic particles (SEPs) also anomalously erupt and accompany solar flares, and are termed solar proton events [81,83]. The SEP and X-ray effects overlap in the sunlit hemisphere. Particles emitted during these events seriously affect the ionosphere and neutral atmosphere, especially in polar regions, resulting in large increases in the concentrations of HO_x (H, OH, HO_2) and NO_x (N, NO, and NO_2) in the mesosphere and stratosphere. They further decrease the ozone concentration [101,83]. SEPs can penetrate the polar D region, which increases the ionization rate there, resulting in enhanced absorption of radio waves in the D region (i.e. polar cap absorption) [102,103].

5 Summary

The ionosphere is mainly produced by solar XUV emissions [6] originating in the chromosphere and corona. The evolution of these emissions is not entirely synchronized [5]. Besides the direct and abrupt response to variations in the XUV ionization, the ionosphere is controlled by chemical, dynamical and electrodynamical processes, which are also modulated by solar activity. Therefore, further investigations are required to better understand and represent the variability of solar activity and its effects on the ionosphere.

Variability in solar activity is embodied in the ionosphere globally, while chemical and dynamical processes vary on different spatial scales. Therefore, we should pay attention to not only global characteristics but also local particularity in the ionosphere variations, particularly during storms. Although both the neutral atmosphere and dynamic factors play critical roles in the ionosphere variations, long-term and global measurements of the thermosphere and neutral winds remain insufficient and need to be expanded. In addition, the polar ionosphere is affected by particle precipitation and Joule heating. The contributions from different factors need to be separated.

In summary, our understanding of the solar activity effects of the ionosphere is increasing with the promotion of

detection approaches and instruments, accumulation of a huge quantity of data, and development of solar radiation and ionospheric models. However, there are still many unresolved problems. For example, what is the relationship of ionospheric parameters with the solar cycle length [104]? In this report, we briefly reviewed recent works. One of the outstanding findings is the existence of linear, saturation and amplification features in the solar activity dependence of the ionosphere. Finally, it should be pointed out that there have been fascinating achievements in the fields of space weather and ionosphere couplings with the lower atmospheres. We have somewhat regretfully limited the scope of this review and not included discussion of those fields.

This work was supported by the National Natural Science Foundation of China (40725014) and the Specialized Research Fund for State Key Laboratories.

1 Pap J, Bouwer S D, Tobiska W K. Periodicities of solar irradiance and solar activity indices. Solar Phys, 1990, 129: 165–189
2 Lundstedt H, Liszka L, Lundin R. Solar activity explored with new wavelet methods. Ann Geophys, 2005, 23: 1505–1511
3 Moussa X, Polygiannakis J M, Preka-Papadema P, et al. Solar cycles: A tutorial. Adv Space Res, 2005, 35: 725–738
4 Lean J. Solar ultraviolet irradiance variations: A review. J Geophys Res, 1987, 92: 839–868
5 Lean J L, White O R, Livingston W C, et al. Variability of a composite chromospheric irradiance index during the 11-year activity cycle and over longer time periods. J Geophys Res, 2001, 106: 10645–10658
6 Gorney D J. Solar cycle effects on the near-earth space environment. Rev Geophys, 1990, 28: 315–336
7 Forbes J M, Bruinsma S, Lemoine F G. Solar rotation effects in the thermospheres of Mars and Earth. Science, 2006, 312: 1366–1368
8 Hinteregger H E, Bedo D E, Manson J E. The EUV spectrophotometer on atmosphere explorer. Radio Sci, 1973, 8: 349–359
9 Ogawa H S, Judge D L, McMullin D R, et al. First-year continuous solar EUV irradiance from SOHO by the CELIAS/SEM during 1996 solar minimum. J Geophys Res, 1998, 103: 1–6
10 Richards P G, Fennelly J A, Torr D G. EUVAC: A solar EUV flux model for aeronomic calculations. J Geophys Res, 1994, 99: 8981–8992
11 Richards P G, Woods T N, Peterson W K. HEUVAC: A new high resolution solar EUV proxy model. Adv Space Res, 2006, 37: 315–322
12 Floyd L, Newmark J, Cook J, et al. Solar EUV and UV spectral irradiances and solar indices. J Atmos Solar-Terr Phys, 2005, 67: 3–15
13 Viereck R A, Puga L, McMullin D, et al. The Mg II index: A proxy for solar EUV. Geophys Res Lett, 2001, 28: 1343–1346
14 Kane R P. Solar EUV and ionospheric parameters: A brief assessment. Adv Space Res, 2003, 32: 1713–1718
15 Tobiska W K, Woods T, Eparvier F, et al. The SOLAR2000 empirical solar irradiance model and forecast tool. J Atmos. Solar-Terr, 2000, 62: 1233–1250
16 Bailey S M, Woods T N, Barth C A, et al. Measurements of the solar soft X-ray irradiance by the Student Nitric Oxide Explorer: First analysis and underflight calibrations. J Geophys Res, 2000, 105: 27179–27193
17 Lean J L, Warren H P, Mariska J T, et al. A new model of solar EUV irradiance variability 2. Comparsions with empirical models and observations and implications for space weather. J Geophys Res, 2003, 108: 1059, doi:10.1029/2001JA009238
18 Bilitza D. The importance of EUV indices for the international reference ionosphere. Phys Chem Earth (C), 2000, 25: 515–521
19 Tobiska W K. Validating the solar EUV proxy, $E_{10.7}$. J Geophys Res, 2001, 106: 29969–29978
20 Barth C A, Tobiska W K, Rottman G J, et al. Comparison of 10.7 cm radio flux with SME solar Lyman-alpha flux. Geophys Res Lett, 1990, 17: 571–574
21 Kane R P. Hysteresis and non-linearity between solar EUV and 10.7 cm fluxes. Ind J Radio Space Phys, 2005, 34: 161–170
22 Kane R P. Fluctuations in the ~27-day sequences in the solar index F10 during solar cycles 22–23. J Atmos Solar-Terr Phys, 2003, 65: 1169–1174
23 Liu L, Wan W, Ning B, et al. Solar activity variations of the ionospheric peak electron density. J Geophys Res, 2006, 111: A08304, doi:10.1029/2006JA011598
24 Liu R, Smith P, King J. A new solar index to improve foF2 prediction using the CCIR Atlas. Telecomm J, 1983, 50: 408–413
25 Ortikov M Yu, Shemelov V A, Shishigin I V, et al. Ionospheric index of solar activity based on the data of measurements of the spacecraft signals characteristics. J Atmos Solar-Terr Phys, 2003, 65: 425–430
26 Mikhailov A, Mikhailov V. A new ionospheric index MF2. Adv Space Res, 1995, 15: 93–97
27 Yue X, Wan W, Liu L, et al. An empirical model of ionospheric foE over Wuhan. Earth Planets Space, 2006, 58: 323–330
28 Nusinov A A. Ionosphere as a natural detector for investigations of solar EUV flux variations. Adv Space Res, 2006, 37: 426–432
29 Afraimovich E L, Astafyeva E I, Oinats A V, et al. Global electron content: A new conception to track solar activity. Ann Geophys, 2008, 26: 335–344
30 Liu L, Wan W, Ning B, et al. Climatology of the mean TEC derived from GPS global ionospheric maps. J Geophys Res, 2009, 114: A06308, doi:10.1029/2009JA014244
31 She C, Wan W, Xu G. Climatological analysis and modeling of the ionospheric global electron content. Chinese Sci Bull, 2008, 53: 282–288
32 Liu R, Xu Z, Wu J, et al. Preliminary studies on ionospheric forecasting in China and its surrounding area. J Atmos Solar-Terr Phys, 2005, 67: 1129–1136
33 Wang J L. Will the solar cycle 24 be a low one? Chinese Sci Bull, 2009, 54: 3664–3668
34 Dikpati M, de Toma G, Gilman P A. Predicting the strength of solar cycle 24 using a flux-transport dynamo-based tool. Geophys Res Lett, 2005, 33: L05102, doi:10.1029/2005GL025221
35 Liu J Y, Chen Y I, Lin J S. Statistical investigation of the saturation effect in the ionospheric foF2 versus sunspot, solar radio noise, and solar EUV radiation. J Geophys Res, 2003, 108: 1067, doi:10.1029/2001JA007543
36 Liu L, Wan W, Ning B. Statistical modeling of ionospheric foF2 over Wuhan. Radio Sci, 2004, 39: RS2013, doi:10.1029/2003RS003005
37 Chen Y, Liu L, Le H. Solar activity variations of nighttime ionospheric peak electron density. J Geophys Res, 2008, 113: A11306, doi:10.1029/2008JA013114
38 Chen Y I, Liu J Y, Chen S C. Statistical investigation of the saturation effect of sunspot on the ionospheric foF2. Phys Chem Earth (C), 2000, 25: 359–362
39 Kane R P. Sunspots, solar radio noise, solar EUV and ionospheric foF2. J Atmos Terr Phys, 1992, 54: 463–466
40 Lei J, Liu L, Wan W, Zhang S R. Variations of electron density based on long-term incoherent scatter radar and ionosonde measurements over Millstone Hill. Radio Sci, 2005, 40: RS2008, doi:10.1029/2004RS003106
41 Mikhailov A V, Mikhailov V V. Solar cycle variations of annual mean noon foF2. Adv Space Res, 1995, 15: 79–82
42 Xu T, Wu Z S, Wu J, et al. Solar cycle variation of the monthly median foF2 at Chongqing station, China. Adv Space Res, 2008, 42: 213–218
43 Richards P G. Seasonal and solar cycle variations of the ionospheric peak electron density: Comparison of measurement and models. J Geophys Res, 2001, 106: 12803–12819

44 Sethi N K, Goel M K, Mahajan K K. Solar cycle variations of foF2 from IGY to 1990. Ann Geophys, 2002, 20: 1677–1685
45 Bhonsle R V, Da Rosa A V, Garriott O K. Measurements of the total electron content and equivalent slab thickness of the mid-latitude ionosphere. Radio Sci, 1965, 69: 929–939
46 Chakraborty S K, Hajra R. Solar control of ambient ionization of the ionosphere near the crest of the equatorial anomaly in the Indian zone. Ann Geophys, 2008, 26: 47–57
47 Huang Y N. Solar cycle variation in the total electron content at Sagamore Hill. J Atoms Terr Phys, 1978, 40: 733–739
48 Liu L, Chen Y. Statistical analysis on the solar activity variations of the TEC derived at JPL from global GPS observations. J Geophys Res, 2009, 114: A10311, doi:10.1029/2009JA014533
49 Titheridge J E. The electron content of the southern mid-latitude ionosphere, 1965–1971. J Atmos Terr Phys, 1973, 35: 981–1001
50 Yeh K C, Flaherty B J. Ionospheric electron content at temperate latitudes during the declining phase of the sunspot cycle. J Geophys Res, 1966, 71: 4557–4570
51 Liu L, Le H, Wan W, et al. An analysis of the scale heights in the lower topside ionosphere based on the Arecibo incoherent scatter radar measurements. J Geophys Res, 2007, 112: A06307, doi: 10.1029/2007JA012250
52 Liu L, Luan X, Wan W, et al. Solar activity variations of equivalent winds derived from global ionosonde data. J Geophys Res, 2004, 109: A12305, doi:10.1029/2004JA010574
53 Liu L, Wan W, Luan X, et al. Solar activity dependence of effective winds derived from ionospheric data at Wuhan. Adv Space Res, 2003, 32: 1719–1924
54 Igi S, Oliver W L, Ogawa T. Solar cycle variations of the thermospheric meridional wind over Japan derived from measurements of h_mF_2. J Geophys Res, 1999, 104: 22427–22431
55 Hedin A E, Buonsanto M J, Codrescu M, et al. Solar activity variations in mid-latitude thermospheric meridional winds. J Gephys Res, 1994, 99: 17601–17608
56 Guo J, Wan W, Forbes J M, et al Effects of solar variability on thermosphere density from CHAMP accelerometer data. J Geophys Res, 2007, 112: A10308, doi:10.1029/ 2007JA012409
57 Liu H, Lühr H, Watanabe S. Climatology of the equatorial thermospheric mass density anomaly. J Geophys Res, 2007, 112: A05305, doi: 10.1029/2006JA012199
58 Balan N, Bailey G J, Jenkins B, et al. Variations of ionospheric ionization and related solar fluxes during an intense solar cycle. J Geophys Res, 1994, 99: 2243–2253
59 Balan N, Bailey G J, Su Y Z. Variations of the ionosphere and related solar fluxes during solar cycles 21 and 22. Adv Space Res, 1996, 18: 11–14
60 Balan N, Bailey G J, Moffett R J. Modeling studies of ionospheric variations during an intense solar cycle. J Geophys Res, 1994, 99: 17467–17475
61 Ma R, Xu J, Wang W, et al. Seasonal and latitudinal differences of the saturation effect between ionospheric NmF2 and solar activity indices. J Geophys Res, 2009, 114: A10303, doi:10.1029/2009JA014353
62 Ortiz de Adler N, Manzano J R. Solar cycle hysteresis on F-region electron concentration peak heights over Tucuman. Adv Space Res, 1995, 15: 83–88
63 Trísková L, Chum J. Hysteresis in dependence of foF2 on solar indices. Adv Space Res, 1996, 18: 145–148
64 Kouris S S, Bradley P A, Dominici P. Solar-cycle variation of the daily foF2 and M(3000)F2. Ann Geophys, 1998, 16: 1039–1042
65 Hedin A E. Correlations between thermospheric density and temperature, solar EUV flux, and 10.7-cm flux variations. J Geophys Res, 1984, 89: 9828–9834
66 Liu H, Stolle C, Förster M, et al. Solar activity dependence of the electron density in the equatorial anomaly regions observed by CHAMP. J Geophys Res, 2007, 112: A11311, doi:10.1029/ 2007JA012616
67 Chen Y, Liu L, Wan W, et al. Solar activity dependence of the topside ionosphere in low latitudes. J Geophys Res, 2009, 114: A08306, doi:10.1029/2008JA013957
68 Liu L, Wan W, Ning B. A study of the ionogram derived effective scale height around the ionospheric hmF2. Ann Geophys, 2006, 24: 851–860
69 Fejer B G, Farley D T, Woodman R F, et al. Dependence of equatorial F-region vertical drifts on season and solar cycle. J Geophys Res, 1979, 84: 5792–5796
70 González S A, Sulzer M P, Nicolls M J, et al. Solar cycle variability of nighttime topside helium ion concentrations over Arecibo. J Geophys Res, 2004, 109: A07302, doi:10.1029/2003JA010100
71 Truhlík V, Třísková L, Šmilauer J. Manifestation of solar activity in the global topside ion composition—A study based on satellite data. Ann Geophys, 2005, 23: 2511–2517
72 West K H, Heelis R A, Rich F J. Solar activity variations in the composition of the low-latitude topside ionosphere. J Geophys Res, 1997, 102: 295–305
73 Kutiev I S, Marinov P G, Watanabe S. Model of topside ionosphere scale height based on topside sounder data. Adv Space Res, 2006, 37: 943–950
74 Zhao B, Wan W, Liu L, et al. Statistical characteristics of the total ion density in the topside ionosphere during the period 1996–2004 using empirical orthogonal function (EOF) analysis. Ann Geophys, 2005, 23: 3615–3631
75 Liu L, Wan W, Yue X, et al. The dependence of plasma density in the topside ionosphere on solar activity level. Ann Geophys, 2007, 25: 1337–1343
76 Liu L, Zhao B, Wan W, et al. Yearly variations of global plasma densities in the topside ionosphere at middle and low latitudes. J Geophys Res, 2007, 112: A07303, doi:10.1029/2007JA012283
77 Su Y Z, Bailey G J, Fukao S. Altitude dependencies in the solar activity variations of the ionospheric electron density. J Geophys Res, 1999, 104: 14879–14891
78 Rich F J, Sultan P J, Burke W J. The 27-day variations of plasma densities and temperatures in the topside ionosphere. J Geophys Res, 2003, 108: 1297, doi:10.1029/2002JA009731
79 Eddy J A. The Maunder minimum. Science, 1976, 192: 1189–1202
80 Smithtro C G, Sojka J J. Behavior of the ionosphere and thermosphere subject to extreme solar cycle conditions. J Geophys Res, 2005, 110: A08306, doi:10.1029/2004JA010782
81 Dmitriev A V, Yeh H C, Chao J K, et al. Top-side ionosphere response to extreme solar events. Ann Geophys, 2006, 24: 1469–1477
82 Tsurutani B T, Gonzalez W D, Lakhina G S, et al. The extreme magnetic storm of 1–2 September 1859. J Geophys Res, 2003, 108: 1268, doi:10.1029/2002JA009504
83 Tsurutani B T, Zambon G A, Guarnieri F L, et al. The October 28, 2003 extreme EUV solar flare and resultant extreme ionospheric effects: Comparison to other Halloween events and the Bastille Day event. Geophys Res Lett, 2005, 32: L03S09, doi:10.1029/2004GL-021475
84 Davies K. Ionospheric Radio. Exeter: Short Run Press Ltd., 1990
85 Mendillo M. Behavior of the ionospheric F region during the greatest solar flare of August 7, 1972. J Geophys Res, 1974, 79: 665–677
86 Wan W, Liu L, Yuan H, et al. The GPS measured SITEC caused by the very intense solar flare on July 14, 2000. Adv Space Res, 2005, 36: 2465–2469
87 Afraimovich E L. GPS global detection of the ionospheric response to solar flares. Radio Sci, 2000, 35: 1417–424
88 Liu H, Lühr H, Watanabe S, et al. Contrasting behavior of the thermosphere and ionosphere in response to the 28 October 2003 solar flare. J Geophys Res, 2007, 112: A07305, doi:10.1029/2007JA012313
89 Chen B, Liu L, Wan W, et al. A statistical analysis of SITEC caused by intense solar flares during 1996–2003 (in Chinese). Chin J Space Sci, 2005, 25: 6–16
90 Liu J Y, Lin C H, Tsai H F, et al. Ionospheric solar flare effects monitored by the ground-based GPS receivers: Theory and observation. J Geophys Res, 2004, 109: A01307, doi:10.1029/2003J- A009931
91 Zhang D H, Xiao Z. Study of the ionospheric TEC using GPS during the large solar flare burst on Nov. 6, 1997. Chinese Sci Bull, 2000, 45: 1749–1752
92 Zhang D H, Xiao Z, Chang Q. The correlation of flare's location on

solar disc and the sudden increase of total electron content. Chinese Sci Bull, 2002, 47: 82–85
93 Zhang D H, Xiao Z. The calculating TEC methods by using GPS observations and their applications for ionospheric disturbances. Chinese Sci Bull, 2000, 43: 451–458
94 Zhang D H, Xiao Z, Igarashi K, et al. GPS-derived ionospheric total electron content response to a solar flare that occurred on 14 July 2000. Radio Sci, 2002, 37: 1086, doi:10.1029/2001RS002542
95 Zhang D H, Xiao Z. Study of the ionospheric total electron content response to the great flare on 15 April 2001 using the International GPS Service network for the whole sunlit hemisphere. J Geophys Res, 2003, 108: 1330, doi:10.1029/2002JA009822
96 Zhang D H, Xiao Z. Study of ionospheric response to the 4B flare on 28 October 2003 using international GPS service network data. J Geophys Res, 2005, 110: A03307, doi:10.1029/2004JA010738
97 Le H, Liu L, Chen B, et al. Modeling the responses of the middle latitude ionosphere to solar flares. J Atmos Solar-Terr Phys, 2007, 69: 1587–1598
98 Huba J D, Warren H P, Joyce G, et al. Global response of the low-latitude to midlatitude ionosphere due to the Bastille Day flare. Geophys Res Lett, 2005, 32: L15103, doi:10.1029/2005GL023291
99 Meier R R, Warren H P, Nicholas A C, et al. Ionospheric and dayglow responses to the radiative phase of the Bastille Day flare. Geophys Res Lett, 2002, 29: 1461, doi:10.1029/2001GL013956
100 Sutton E K, Forbes J M, Nerem R S, et al. Neutral density response to the solar flares of October and November, 2003. Geophys Res Lett, 2006, 33: L22101, doi:10.1029/2006GL027737
101 Jackman C H, DeLand M T, Labow G J, et al. Influence of several very large solar proton events in years 2000–2003 on the neutral middle atmosphere. Adv Space Res, 2005, 35: 445–450
102 Shea M A, Smart D F. A summary of major solar proton events. Solar Physics, 1990, 127: 297–320
103 Osepian A, Kirkwood S, Dalin P. The influence of ozone concentration on the lower ionosphere – Modelling and measurements during the 29–30 October 2003 solar proton event. Ann Geophys, 2009, 27: 577–589
104 de Adler N O, Elías A G, Manzano J R. Solar cycle length variation: Its relation with ionospheric parameters. J Atmos Solar-Terr Phys, 1997, 59: 159–162